



Lecture Notes in Mechanical Engineering

Shankar Krishnapillai
Velmurugan R.
Sung Kyu Ha *Editors*

Composite Materials for Extreme Loading

Proceedings of the Indo-Korean
workshop on Multi Functional Materials
for Extreme Loading 2021



Springer

Shankar Krishnapillai · Velmurugan R. ·
Sung Kyu Ha
Editors

Composite Materials for Extreme Loading

Proceedings of the Indo-Korean workshop
on Multi Functional Materials for Extreme
Loading 2021

Parametric Analysis and Response Surface Optimization of Surface Roughness and Cutting Rate in the Machining Using WEDM



I. V. Manoj and S. Narendranath

Abstract Nickelvax HX is an amalgamation of nickel, chromium, iron, molybdenum etc. As nickel-based alloys have high-temperature strength they can be used in many applications like afterburners, blades of turbines, turbochargers, submarines parts etc. Wire electric discharge machining a non-contact spark machining was found to be the most precise machining process. Among the WEDM parameters, different process parameters like servo voltage, pulse on time, cutting speed override and pulse off time were employed for the examination. It was noticed that both response characteristics increased with the increase in cutting speed override and pulse on-time. In the case of servo voltage and pulse off time, as it was increased the cutting rate and surface roughness diminished. The effects of cutting rate on surface roughness and microhardness were analyzed. The response surface optimization was employed for optimizing surface roughness and cutting rate as it controls product quality.

Keywords Response surface methodology · Wire electric discharge machining · Cutting rate · Surface roughness

1 Introduction

Nickel base alloy possesses excellent high-temperature strength and high mechanical properties. It can be used in petrochemical, aerospace, marine, nuclear industries etc. [1, 2]. The high-temperature strength and thermal diffusivity lead to damage in both the tool and workpiece. Wire electric discharge machining (WEDM) is a spark erosive method, where the spark melts and evaporates the alloy proved to be the most promising machining solutions available in the market for nickel-based alloys [3, 4]. As WEDM possesses many parameters, it becomes a necessity for finding favourable characteristics for machining many optimization techniques have been employed for machining different alloys.

I. V. Manoj (✉) · S. Narendranath
Department of Mechanical Engineering, National Institute of Technology Karnataka,
Surathkal, India

Reolon et al. [5] concluded that zinc-coated copper wire performed better than uncoated brass wire for all the experiments during WEDM machining of IN718. Manoj et al. [6, 7] attempted to investigate different effects of cutting speed during machining of Hastelloy-X. Soni et al. [8] explored grey relational analysis methods for formulating and optimization of surface roughness and material removal rate in WEDM of shape memory alloys. Manjaiah et al. [9] have found optimal parameters that yields minimized surface roughness and maximized material removal rate while WEDM of pure titanium. It was found that machining responses were not influenced by servo voltage and wire speed during optimization. Kumar et al. [10] proved cryo-treated brass wire gives improved performance using response surface methodology during wire EDM and there was an increase in 102% and 35% in the cutting speed and surface roughness. Bose and Nandi [11] have reported multi-objective optimization using response surface methodology and desirability of 0.72 was obtained from this multi-objective optimized solution. Sarkar et al. [12] have combined the machining strategy of both single and multi-pass cutting, giving the new concept of effective cutting speed for WEDM of gamma titanium aluminide. Chaudhari et al. [13] analysed with the aid of the RSM–GRA integrated approach for optimal parameter setting for the WEDM process. This optimal setting maximized the cutting rate while decreasing surface roughness during the machining of pure titanium. Kumar et al. [14] have reported optimal cutting speed and kerf width using Response surface methodology (RSM) in the machining of AlSiCeB4C composites with input parameters like wire feed rate, pulse on time, current and different combination of the content of B4C in aluminium. Muralidharan et al. [15] investigated machining of AA2024/ZrB2 cast composites where minimum surface roughness and maximum material removal rate were achieved using RSM. Bhartiya et al. [16] investigated machining of Si wafers by response surface methodology using multi-objective optimization to achieve minimum kerf-loss. Hamed et al. [17] reported analysis and predicting parameter using the response surface method for output parameters like surface roughness, white layer thickness and depth of heat affected zone in WEDM. Soundararajan et al. [18] have employed response surface methodology for optimizing surface roughness and metal removal rate in the machining of cast A413–B4C composites.

From the above literature, we can conclude that the quantity of a machined product depends on the rate of cutting and surface roughness. RSM can be utilized for the analysis and optimization of machining parameters. In the present investigation surface roughness and cutting rate is optimized using zinc-coated copper wire for machining of Nickelvax HX. RSM is employed to find the optimal machining responses for input parameters like pulse off time (T_{off}), cutting speed override (CSO), pulse on time (T_{on}) and servo voltage (SV) on Nickelvax HX. With the increase in pulse on time and cutting speed override increase both response parameters increases. The increase in servo voltage and pulse off time decreases the response characteristics. Surface roughness and micro-hardness variation with the rate of cutting were investigated. Using response surface optimization is performed to get the favourable cutting rate and surface roughness.

Table 1 Composition of Nickelvax HX

| % | C% | Si% | Mn% | P% | S% | Cr% | Mo% | Fe% | Co% | W% | Ni% |
|-------------|------|------|------|-------|------|-------|------|-------|------|------|-------|
| Composition | 0.06 | 0.21 | 0.65 | 0.027 | 0.01 | 20.65 | 8.24 | 18.05 | 0.69 | 0.29 | 50.88 |

2 Material

Hastelloy-X/Nickelvax HX is a superalloy having high mechanical properties, oxidation resistance, fabricability and high-temperature strength. The composition is shown in Table 1. This was tested and verified using optical emission spectrometry (SpectraMax 130,779). The alloy was solution heat-treated at 2150 °F (1177 °C) (Hold at temperature for a maximum of 30 min, for sheet and 1 h per inch of thickness).

3 Experimental Particulars

The Electronica 'ELPLUS 15 CNC WEDM' was employed in the machining of Nick-elvac HX. The zinc-coated copper acts as the electrode. This electrode is surrounded by dielectric fluid throughout the machining. The dielectric fluid not only acts as a medium for the ionisation process but also cools the work material and carries away the debris formed during melting. As the workpiece and electrode were maintained at the higher voltage the ionisation occurs and the spark generates. This hits the work-piece and melts the material. Figure 1(a) shows the material placed on the WEDM

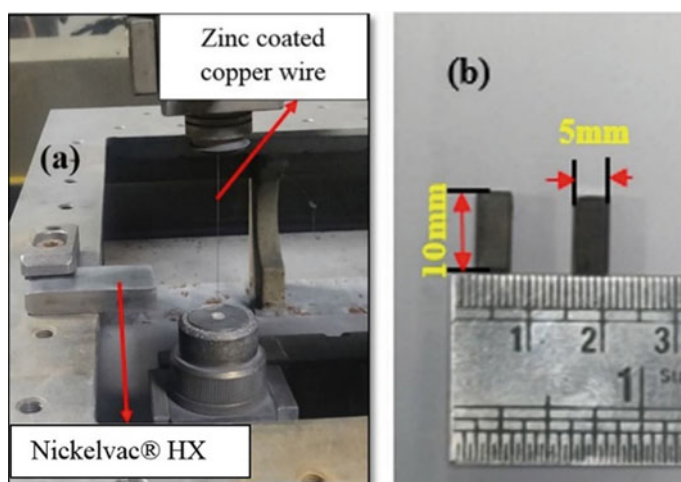


Fig. 1 a Nickelvac HX fixed in WEDM table b Machined workpiece considered for investigation

Table 2 Constant machining parameters

| Parameter | Setting |
|--------------------------|-----------------|
| Wire feed (m/min) | 5 |
| Servo feed (mm/min) | 20 |
| Wire guide distance (mm) | 60 |
| Dielectric fluid | Deionized water |
| Polarity | Positive |
| Electrode (Wire) | Negative |
| Workpiece | Positive |

Table 3 Parameters used for investigation

| Parameters | Level 1 | Level 2 | Level 3 |
|--|---------|---------|---------|
| Pulse on time (T_{on}) (μs) | 115 | 120 | 125 |
| Pulse off time (T_{off}) (μs) | 30 | 45 | 60 |
| Servo voltage (SV) (V) | 30 | 45 | 60 |
| Cutting speed override (CSO) (%) | 40 | 60 | 80 |

table used for machining and Fig. 1(b) shows different specimens machined from the workpiece.

4 Parameters

The initial experiment was conducted for the wire and material combination with constant parameters as shown in Table 2. The wire material was zinc-coated copper having a diameter of 0.25 mm. The machinable parameters and machining capabilities the parameters were selected for the response surface methodology. Based on the literature response surface method was employed for optimization. The Box–Behnken (BB) design was utilized and experiments conducted for different parametric combinations. Table 3 shows the different parameters chosen for RSM.

5 Results and Discussion

Based on the RSM the machining was performed on the material for different process parameters as shown in Table 4. The cutting rate was calculated as the average of all instantaneous cutting speeds obtained from the WEDM machine. The cutting speed is defined as the length of cut in mm per time in minutes [19]. The surface roughness was measured as the average of 5 Ra values of the machined surface. It was

Table 4 Rate of cutting and surface roughness for different combinations of parameters

| Sl. No. | Pulse on time (μs) T_{on} | Pulse off time (μs) T_{off} | Servo voltage (V) SV | Cutting speed override (%) CSO | Cutting rate (mm/min) | Surface roughness (μm) |
|---------|---------------------------------------|---|-------------------------|-----------------------------------|-----------------------|-------------------------------|
| 1 | 115 | 30 | 45 | 60 | 1.187 | 2.457 |
| 2 | 120 | 45 | 30 | 40 | 1.354 | 3.383 |
| 3 | 115 | 45 | 45 | 80 | 0.961 | 2.297 |
| 4 | 120 | 60 | 30 | 60 | 0.717 | 2.190 |
| 5 | 120 | 60 | 45 | 40 | 1.151 | 2.303 |
| 6 | 120 | 45 | 60 | 40 | 0.570 | 2.267 |
| 7 | 120 | 30 | 60 | 60 | 1.313 | 2.807 |
| 8 | 125 | 45 | 45 | 40 | 0.900 | 1.670 |
| 9 | 120 | 45 | 30 | 80 | 2.560 | 3.310 |
| 10 | 115 | 45 | 45 | 40 | 1.314 | 2.710 |
| 11 | 125 | 30 | 45 | 60 | 1.858 | 3.443 |
| 12 | 120 | 45 | 45 | 60 | 0.512 | 1.350 |
| 13 | 120 | 45 | 45 | 60 | 1.855 | 3.563 |
| 14 | 115 | 45 | 60 | 60 | 1.640 | 2.760 |
| 15 | 120 | 30 | 30 | 60 | 0.720 | 1.673 |
| 16 | 125 | 45 | 45 | 80 | 1.332 | 2.790 |
| 17 | 115 | 60 | 45 | 60 | 0.558 | 1.700 |
| 18 | 125 | 45 | 60 | 60 | 0.785 | 1.900 |
| 19 | 120 | 60 | 60 | 60 | 0.610 | 1.873 |
| 20 | 120 | 30 | 45 | 40 | 1.409 | 2.517 |
| 21 | 120 | 45 | 45 | 60 | 1.254 | 2.970 |
| 22 | 115 | 45 | 30 | 60 | 1.296 | 2.327 |
| 23 | 125 | 60 | 45 | 60 | 1.608 | 3.297 |
| 24 | 115 | 30 | 45 | 60 | 0.980 | 2.357 |
| 25 | 120 | 45 | 30 | 40 | 0.822 | 1.697 |
| 26 | 115 | 45 | 45 | 80 | 1.222 | 2.373 |
| 27 | 120 | 60 | 30 | 60 | 1.555 | 3.247 |

recorded with the aid of the ‘Mitutoyo SJ-301’ surface roughness tester. The surface roughness varies from 1.35 to 3.56 μm and the rate of cutting varies from 0.51 to 2.56 mm/min. Equations 1 and 2 shows the regression equation for the response parameters recorded at different parameters.

Regression Equation for Cutting rate

$$MS (mm/min) = -1.23 - 0.0224 T_{on} - 0.00856 T_{off} + 0.01070 SV - 0.01045 CSO \quad (1)$$

Regression Equation for surface roughness

$$SR(Ra) = -1.20 + 0.0315 T_{on} - 0.051 T_{off} + 0.0079 SV - 0.0088 CSO \quad (2)$$

5.1 Influence of Machining Parameters on Response Characteristics

In the surface plot indicated in Fig. 2(a), it can be established that as T_{on} increases the cutting rate also escalates. With the increase in the cutting rate, the sparking that occurs at the workpiece and wire interface during machining also increases. This intensifies the discharge energy, which results in faster melting of the material, which in turn increases the length of the kerf. So the cutting rate escalates as the T_{on} increases. In the case of T_{off} , as it increases the cutting rate decreases. This is due to the decrease in sparking at the wire and workpiece interface. This leads to lower discharge energy which experiences a lower melting rate at the wire and material interface. This decreases the cutting rate as shown in Fig. 2(a). Similar effects of machining parameters were observed in Sharma et al. [20] and Kumar et al. [21]. Both the parameters T_{on} and T_{off} controls the discharge energy that influences the melting of the material.

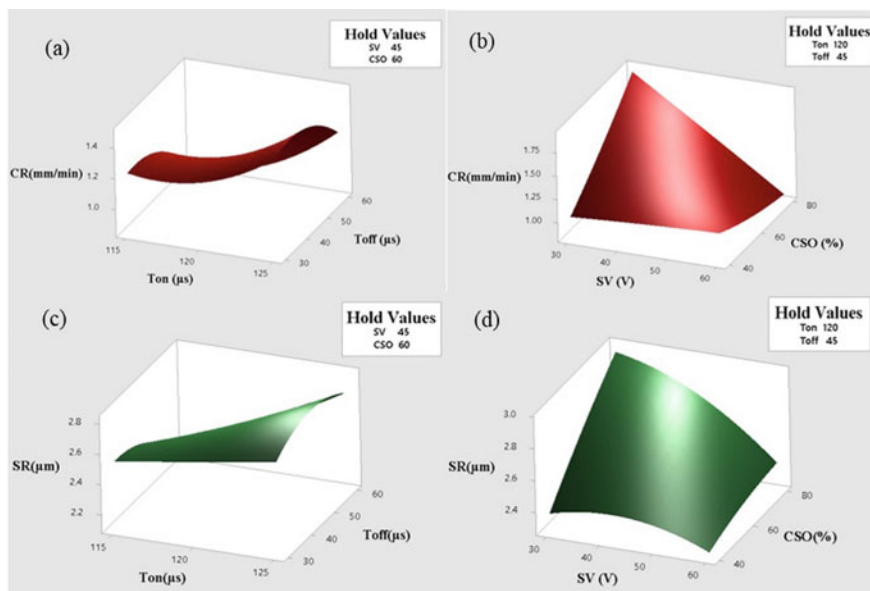


Fig. 2 Behaviour of a, b cutting rate and c, d surface roughness

From Fig. 2(b) the variation of cutting rate with SV and CSO can be seen. The SV controls the gap between the workpiece and the wire. At lower values of SV, the gap is smaller this helps the material melt faster due to the increase in discharge energy. This increases the discharge energy, therefore the cutting rate at lower SV increases. At higher SV, the gap at wire and workpiece interface increases which decreases the discharge energy. Comparable results were witnessed in Kumar et al. [21]. As the gap increases the sparks at the wire workpiece junction will be lower leading to lower discharge energy and lower cutting rate. In the case of CSO, it is used for complex profiles as it is an override parameter it can control the cutting rate without altering the set parameters. As CSO increases the cutting rate also increases. The CSO dictates the discharge energy created at the wire and workpiece interface. The higher the CSO, the higher will be the discharge energy. So the cutting rate also increases as shown in Fig. 2(b). Manoj et al. [22, 23] have also observed similar results during profiling.

The surface roughness was also measured and analyzed as indicated in Fig. 2(c) and (d). As T_{on} increases the sparks increases due to which the discharge increases. The number of sparks hitting the workpiece also escalates. This creates larger and deeper craters increasing the surface roughness on the machined surface [20]. So as T_{on} increases the surface roughness also increases. In the case of T_{off} , the sparks hitting the workpiece decreases forming shallower and smaller craters on the machined surface. So the surface roughness at higher T_{off} parameter decreases [20, 21]. A similar analogy is observed at SV also as it increases the gap increases between the workpiece and wire. This decreases the number of sparks striking the workpiece [21]. Therefore it forms shallower and smaller craters on the WEDMed surface decreasing the surface roughness. At lower SV the gap is smaller the sparks at the workpiece and wire is higher resulting in larger and deeper craters. This increases the surface roughness on the WEDMed surface. In the case of CSO, the CSO is the override parameter as it is increased the discharge energy is higher [22, 23]. The sparks generated at the wire and workpiece interface will increase which increases the surface roughness. At lower CSO the discharge will be lesser where the craters formed on the WEDMed surface will be smaller. So the surface roughness is lower.

5.2 Optimization of Cutting Rate and Surface Roughness

The optimization was performed using MINITAB software as shown in Fig. 3. Based on the responses in Table 4 the surface roughness was minimized and the cutting rate was maximized. This was also confirmed experimentally as shown in Table 5. The percentage error noticed were 9.09% and 7.81% for cutting rate and surface roughness respectively. Fig. 4 represents the variation of surface roughness with cutting rate. It can be observed that as the cutting rate increases the surface roughness also increases as Fig. 2(d).

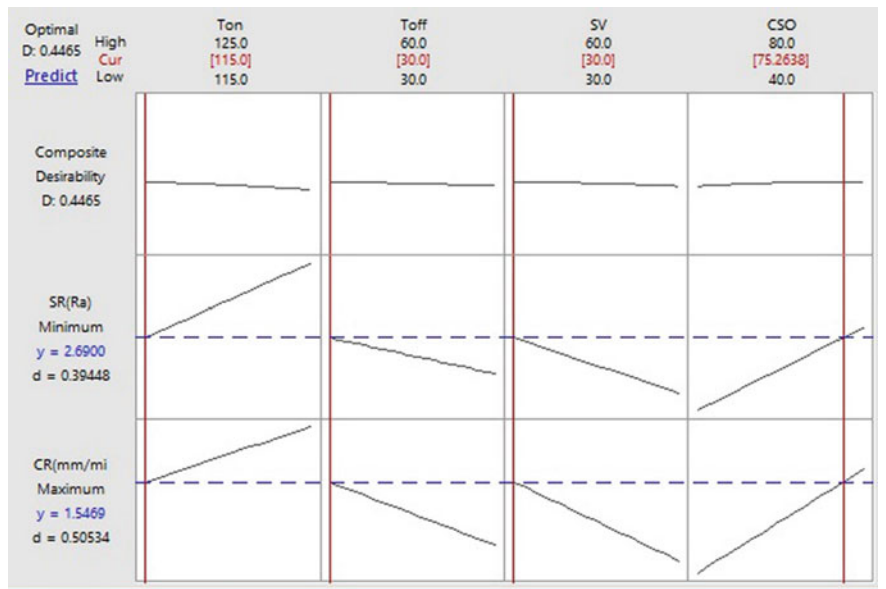


Fig. 3 Optimized response generated from Minitab

Table 5 Optimal parameters and conformational experimental Tests

| Sl. No | Pulse on time (μ s) T_{on} | Pulse off time (μ s) T_{off} | Servo voltage (V) SV | Cutting speed override (%) CSO | Cutting rate (mm/min) | | Surface roughness (μ m) | |
|--------|--------------------------------------|--|----------------------|--------------------------------|-----------------------|------------|------------------------------|------------|
| | | | | | Experimental | RSM values | Experimental | RSM values |
| 1 | 115 | 30 | 30 | 75 | 1.54 | 1.40 | 2.69 | 2.91 |

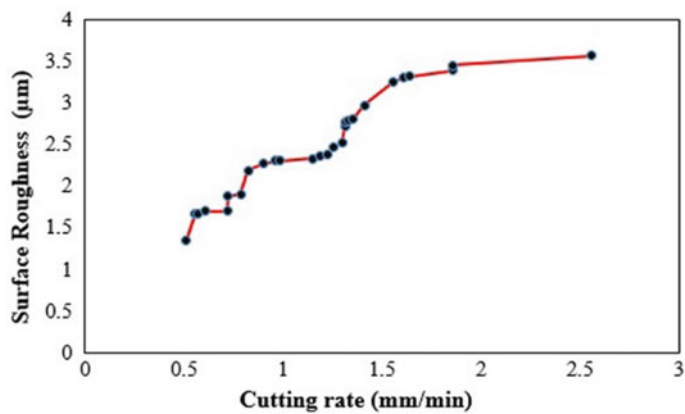
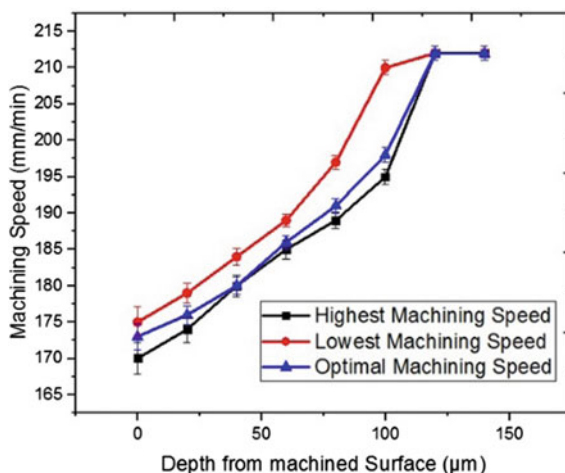


Fig. 4 Influence of the rate of cutting on surface roughness

Fig. 5 Micro-hardness analysis for different cutting rate WEDMed surface



5.3 Variation of Surface Roughness and Micro-hardness

From Fig. 2 different variations in the cutting rate and surface roughness was observed. It can be witnessed that at the higher cutting rate the surface roughness is also higher. At higher cutting rates, the sparks near the wire and workpiece interface. This increases the crater or micro-holes formed on the machined workpiece. Therefore the surface roughness increases at the higher cutting rate and also other researchers have observed surface roughness behaviour in the same manner [6–8].

The micro-hardness was measured at highest (2.56 mm/min), lowest (0.717 mm/min) and optimal (1.547 mm/min) cutting rates WEDMed surface as in Fig. 5. It was performed using ‘OMNI TECH MVHS-AUTO’ Vicker’s micro-hardness tester. The average micro-hardness of five values were considered for analysis. It was observed as the hardness of the highest cutting rate was lower than that of the lowest cutting rate. This was due to the effect of heat at the WEDMed surface. At a higher cutting rate, the discharge energy is more and the heat generated is also more. This leads to more thermal degradation of the material. The material in turn softens giving lower hardness compared to the lowest cutting rate. It noted that the optimal cutting rate gave a hardness in between the hardness of lower and higher cutting rate. Similar results were noted in Joy et al. [7].

6 Conclusion

In the above study, RSM was employed for machining of Nickelvax HX where the influence of machining parameters on responses was analyzed and optimized for the first time. As the T_{on} and CSO escalate both surface roughness and the cutting rate increased. Whereas the SV and T_{off} parameters affected adversely on the response

parameter. The optimal parameters were 115(T_{on}), 30(T_{off}), 30(SV), 75(CSO) and the experimental response compared with RSM optimal response parameters yielded 7.81–9.09% error. As the cutting rate increases from 0.51 to 2.56 mm/min, the surface roughness also increases from 1.35 to 3.56 Ra. The lowest hardness is found in the highest cutting rate WEDMed surface having 167HV and optimal cutting rate yielded the hardness of 170 HV which was found in between the highest and lowest cutting rate hardness.

References

1. Henderson MB, Arrell D, Larsson R, Heobel M, Marchant G (2004) Nickel based superalloy welding practices for industrial gas turbine applications. *Sci Technol Weld Joining* 9(1):13–21
2. Ezugwua EO, Wanga ZM, Machadob AR (1999) The machinability of nickel-based alloys: a review. *J Mater Process Technol* 86(1–3):1–16
3. Manoj IV, Joy R, Narendranath S, Nedelcu D (2019) Investigation of machining parameters on corner accuracies for slant type taper triangle shaped profiles using WEDM on Hastelloy X. *IOP Conf Ser Mater Sci Eng* 591(1):1–11
4. Nayak BB, Mahapatra SS (2016) Optimization of WEDM process parameters using deep cryo-treated Inconel 718 as work material. *Eng Sci Technol Int J* 19(1):161–170
5. Reolon LW, Henning Laurindo CA, Torres RD, Amorim FL (2019) WEDM performance and surface integrity of Inconel alloy IN718 with coated and uncoated wires. *Int J Adv Manuf Technol* 100:1981–1991
6. Manoj IV, Joy R, Narendranath S (2020) Investigation on the effect of variation in cutting speeds and angle of cut during slant type taper cutting in WEDM of Hastelloy X. *Arab J Sci Eng* 45(2):641–651
7. Joy R, Manoj IV, Narendranath S (2020) Investigation of cutting speed, recast layer and micro-hardness in angular machining using slant type taper fixture by WEDM of Hastelloy X. *Mater Today Proc* 27:1943–1946
8. Hargovind S, Narendranath S, Ramesh MR (2019) Advanced machining of TiNiCo shape memory alloys for biomedical applications. *Emerg Mater Res* 8(1):14–21
9. Manjaiah M, Narendranath S, Basavarajappa S, Gaitonde VN (2014) Wire electric discharge machining characteristics of titanium nickel shape memory alloy. *Trans Nonferrous Metals Soc China* 24(10):3201–3209
10. Kumar A, Sharma R, Gujral R (2021) Multi-objective optimization and surface morphology of M-42 AISI steel using normal and cryo-treated brass wire in wire cut. *EDM Arab J Sci Eng*. <https://doi.org/10.1007/s13369-020-05204-z>
11. Bose S, Nandi T (2021) Parametric optimization of WEDM on hybrid titanium matrix composite using response surface methodology. *Multis Multidisc Model Exp Des*. <https://doi.org/10.1007/s41939-020-00088-w>
12. Sarkar S, Ghosh K, Mitra S, Bhattacharyya B (2010) An integrated approach to optimization of WEDM combining single-pass and multipass cutting operation. *Mater Manuf Processes* 25(8):799–807. <https://doi.org/10.1080/10426910903575848>
13. Chaudhari R, Vora J, Parikh DM, Wankhede V, Khanna S (2020) Multi-response optimization of WEDM parameters using an integrated approach of RSM–GRA analysis for pure titanium. *J Inst Eng (India) Ser D* 101:117–126
14. Suresh Kumar S, Erdemir F, Varol T, Thirumalai Kumaran S, Uthayakumar M, Canakci A (2020) Investigation of WEDM process parameters of AlSiCeB4C composites using response surface methodology. *Int J Lightweight Mater Manuf* 3:127–135

15. Muralidharan N, Chockalingam K, Parameshwaran R, Kalaiselvan K, Nithyavathy N (2020) Optimization of CNC-WEDM parameters for AA2024/ZrB2 in situ stir cast composites using response surface methodology with desirability function technique. *Arab J Sci Eng* 45:5563–5579. <https://doi.org/10.1007/s13369-020-04490-x>
16. Rana P, Bhartiya D, Annebushan Singh M, Marla D (2020) Multi-objective optimization of wire electrical discharge machined ultra-thin silicon wafers using response surface methodology for solar cell applications. In: *Proceedings of the ASME 2020 15th international manufacturing science and engineering, manufacturing processes; manufacturing systems; nano/micro/meso manufacturing*, vol 2, pp 1–7. *Quality and Reliability*. Virtual, Online. V002T08A021. ASME. <https://doi.org/10.1115/MSEC2020-8489>
17. Hamed S, Al-Juboori LA, Najm VN, Saleh AM (2020) Analysis the impact of WEDM parameters on surface microstructure using response surface methodology. In: *Advances in science and engineering technology international conferences (ASET)*, Dubai, United Arab Emirates, pp 1–8. <https://doi.org/10.1109/ASET48392.2020.9118208>
18. Soundararajan R, Ramesh A, Ponappa K, Sivasankaran S, Arvind D (2020) Optimization of WEDM process parameters by RSM in machining of stir cum squeeze cast A413–B4C composites. *SN Appl Sci* 1768(2). <https://doi.org/10.1007/s42452-020-03409-3>
19. Azam M, Jahanzaib M, Abbasi JA, Wasim A (2016) Modeling of cutting speed (CS) for HSLA steel in wire electrical discharge machining (WEDM) using moly wire. *J Chinese Inst Eng* 39(7):802–808
20. Sharma P, Chakradhar D, Narendranath S (2015) Evaluation of WEDM performance characteristics of Inconel 706 for turbine disk application. *Mater Des* 88:558–566
21. Kumar V, Kumar V, Jangra KK (2015) An experimental analysis and optimization of machining rate and surface characteristics in WEDM of Monel-400 using RSM and desirability approach. *J Ind Eng Int* 11:297–307
22. Manoj IV, Narendranath S (2020) Variation and artificial neural network prediction of profile areas during slant type taper profiling of triangle at different machining parameters on Hastelloy X by wire electric discharge machining. *Proc Inst Mech Eng Part E J Process Mech Eng* 234(6):673–683
23. Manoj IV, Narendranath S (2020) Influence of machining parameters on taper square areas during slant type taper profiling using wire electric discharge machining. *IOP Conf Ser Mater Sci Eng* 1017(1):1–9